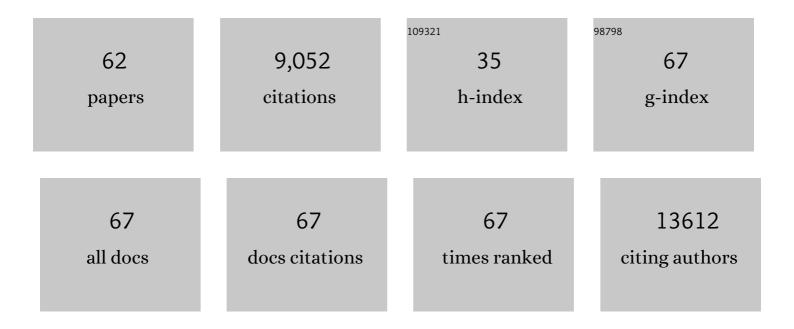
List of Publications by Year in descending order

Source: https://exaly.com/author-pdf/4903770/publications.pdf Version: 2024-02-01



Κυμανιζιμη ΔΝ

#	Article	IF	CITATIONS
1	Boosting Support Reducibility and Metal Dispersion by Exposed Surface Atom Control for Highly Active Supported Metal Catalysts. ACS Catalysis, 2022, 12, 4402-4414.	11.2	19
2	Boosting Thermal Stability of Volatile Os Catalysts by Downsizing to Atomically Dispersed Species. Jacs Au, 2022, 2, 1811-1817.	7.9	4
3	Complete utilization of waste lignin: preparation of lignin-derived carbon supports and conversion of lignin-derived guaiacol to nylon precursors. Catalysis Science and Technology, 2022, 12, 5021-5031.	4.1	3
4	Interfacial effect of Pd supported on mesoporous oxide for catalytic furfural hydrogenation. Catalysis Today, 2021, 365, 291-300.	4.4	13
5	Cu2O(100) surface as an active site for catalytic furfural hydrogenation. Applied Catalysis B: Environmental, 2021, 282, 119576.	20.2	43
6	Modified Metal–Organic Frameworks as Efficient Catalysts for Lignocellulosic Biomass Conversion. Bulletin of the Korean Chemical Society, 2021, 42, 346-358.	1.9	5
7	Atomically Alloyed Fe–Co Catalyst Derived from a N-Coordinated Co Single-Atom Structure for CO <sub>2</sub> Hydrogenation. ACS Catalysis, 2021, 11, 2267-2278.	11.2	48
8	Methane oxidation to formaldehyde over vanadium oxide supported on various mesoporous silicas. Korean Journal of Chemical Engineering, 2021, 38, 1224-1230.	2.7	5
9	Layered Double Hydroxide-Derived Intermetallic Ni <sub>3</sub> GaC <sub>0.25</sub> Catalysts for Dry Reforming of Methane. ACS Catalysis, 2021, 11, 11091-11102.	11.2	26
10	Revealing Charge Transfer at the Interface of Spinel Oxide and Ceria during CO Oxidation. ACS Catalysis, 2021, 11, 1516-1527.	11.2	20
11	Influence of the Pt size and CeO <sub>2</sub> morphology at the Pt–CeO <sub>2</sub> interface in CO oxidation. Journal of Materials Chemistry A, 2021, 9, 26381-26390.	10.3	28
12	Highly dispersed Pd catalysts supported on various carbons for furfural hydrogenation. Catalysis Today, 2020, 350, 71-79.	4.4	30
13	Structural evolution of ZIF-67-derived catalysts for furfural hydrogenation. Journal of Catalysis, 2020, 392, 302-312.	6.2	25
14	Recycling Carbon Dioxide through Catalytic Hydrogenation: Recent Key Developments and Perspectives. ACS Catalysis, 2020, 10, 11318-11345.	11.2	215
15	Al2O3-Coated Ni/CeO2 nanoparticles as coke-resistant catalyst for dry reforming of methane. Catalysis Science and Technology, 2020, 10, 8283-8294.	4.1	22
16	Cobalt Ferrite Nanoparticles to Form a Catalytic Co–Fe Alloy Carbide Phase for Selective CO <sub>2</sub> Hydrogenation to Light Olefins. ACS Catalysis, 2020, 10, 8660-8671.	11.2	95
17	An efficient hydrogenation catalytic model hosted in a stable hyper-crosslinked porous-organic-polymer: from fatty acid to bio-based alkane diesel synthesis. Green Chemistry, 2020, 22, 2049-2068.	9.0	61
18	Synergistic effect of quinary molten salts and ruthenium catalyst for high-power-density lithium-carbon dioxide cell. Nature Communications, 2020, 11, 456.	12.8	39

#	Article	IF	CITATIONS
19	Structure-dependent catalytic properties of mesoporous cobalt oxides in furfural hydrogenation. Applied Catalysis A: General, 2019, 583, 117125.	4.3	22
20	Enhanced hot electron generation by inverse metal–oxide interfaces on catalytic nanodiode. Faraday Discussions, 2019, 214, 353-364.	3.2	13
21	Integration of Interfacial and Alloy Effects to Modulate Catalytic Performance of Metal–Organic-Framework-Derived Cu–Pd Nanocrystals toward Hydrogenolysis of 5-Hydroxymethylfurfural. ACS Sustainable Chemistry and Engineering, 2019, 7, 10349-10362.	6.7	83
22	Mesoporous mixed CuCo oxides as robust catalysts for liquid-phase furfural hydrogenation. Applied Catalysis A: General, 2019, 571, 118-126.	4.3	37
23	Catalytic 1-Propanol Oxidation on Size-Controlled Platinum Nanoparticles at Solid–Gas and Solid–Liquid Interfaces: Significant Differences in Kinetics and Mechanisms. Journal of Physical Chemistry C, 2019, 123, 7577-7583.	3.1	8
24	Supported Pd nanoparticle catalysts with high activities and selectivities in liquid-phase furfural hydrogenation. Fuel, 2018, 226, 607-617.	6.4	60
25	Catalytic CO Oxidation on Nanocatalysts. Topics in Catalysis, 2018, 61, 986-1001.	2.8	15
26	Specific Metal–Support Interactions between Nanoparticle Layers for Catalysts with Enhanced Methanol Oxidation Activity. ACS Catalysis, 2018, 8, 5391-5398.	11.2	63
27	Catalytic CO Oxidation over Au Nanoparticles Supported on CeO <sub>2</sub> Nanocrystals: Effect of the Au–CeO <sub>2</sub> Interface. ACS Catalysis, 2018, 8, 11491-11501.	11.2	173
28	SiO2@V2O5@Al2O3 core–shell catalysts with high activity and stability for methane oxidation to formaldehyde. Journal of Catalysis, 2018, 368, 134-144.	6.2	19
29	Chemically impregnated NiO catalyst for molten electrolyte based gas-tank-free Li O2 battery. Journal of Power Sources, 2018, 402, 68-74.	7.8	11
30	Acidic effect of porous alumina as supports for Pt nanoparticle catalysts in n-hexane reforming. Catalysis Science and Technology, 2018, 8, 3295-3303.	4.1	16
31	Boosting hot electron flux and catalytic activity at metal–oxide interfaces of PtCo bimetallic nanoparticles. Nature Communications, 2018, 9, 2235.	12.8	80
32	Transition Metal-Based Thiometallates as Surface Ligands for Functionalization of All-Inorganic Nanocrystals. Chemistry of Materials, 2017, 29, 10510-10517.	6.7	13
33	Postsynthesis Modulation of the Catalytic Interface inside a Hollow Nanoreactor: Exploitation of the Bidirectional Behavior of Mixed-Valent Mn <sub>3</sub> O <sub>4</sub> Phase in the Galvanic Replacement Reaction. Chemistry of Materials, 2016, 28, 9049-9055.	6.7	21
34	Photocatalytic H <sub>2</sub> generation on macro-mesoporous oxide-supported Pt nanoparticles. RSC Advances, 2016, 6, 18198-18203.	3.6	14
35	High-performance hybrid oxide catalyst of manganese and cobalt for low-pressure methanol synthesis. Nature Communications, 2015, 6, 6538.	12.8	135
36	Nanocatalysis I: Synthesis of Metal and Bimetallic Nanoparticles and Porous Oxides and Their Catalytic Reaction Studies. Catalysis Letters, 2015, 145, 233-248.	2.6	120

#	Article	IF	CITATIONS
37	Hollow MnOxPy and Pt/MnOxPy yolk/shell nanoparticles as a T1 MRI contrast agent. Journal of Colloid and Interface Science, 2015, 439, 134-138.	9.4	7
38	Evidence of Highly Active Cobalt Oxide Catalyst for the Fischer–Tropsch Synthesis and CO <sub>2</sub> Hydrogenation. Journal of the American Chemical Society, 2014, 136, 2260-2263.	13.7	211
39	Effects of Nanoparticle Size and Metal/Support Interactions in Pt-Catalyzed Methanol Oxidation Reactions in Gas and Liquid Phases. Catalysis Letters, 2014, 144, 1930-1938.	2.6	34
40	Comparing the Catalytic Oxidation of Ethanol at the Solid–Gas and Solid–Liquid Interfaces over Size-Controlled Pt Nanoparticles: Striking Differences in Kinetics and Mechanism. Nano Letters, 2014, 14, 6727-6730.	9.1	45
41	High-Temperature Catalytic Reforming of <i>n</i> -Hexane over Supported and Core–Shell Pt Nanoparticle Catalysts: Role of Oxide–Metal Interface and Thermal Stability. Nano Letters, 2014, 14, 4907-4912.	9.1	69
42	Designed Catalysts from Pt Nanoparticles Supported on Macroporous Oxides for Selective Isomerization of <i>n</i> -Hexane. Journal of the American Chemical Society, 2014, 136, 6830-6833.	13.7	100
43	Promotion of Hydrogenation of Organic Molecules by Incorporating Iron into Platinum Nanoparticle Catalysts: Displacement of Inactive Reaction Intermediates. ACS Catalysis, 2013, 3, 2371-2375.	11.2	22
44	Enhanced CO Oxidation Rates at the Interface of Mesoporous Oxides and Pt Nanoparticles. Journal of the American Chemical Society, 2013, 135, 16689-16696.	13.7	361
45	Preparation of mesoporous oxides and their support effects on Pt nanoparticle catalysts in catalytic hydrogenation of furfural. Journal of Colloid and Interface Science, 2013, 392, 122-128.	9.4	90
46	Influence of Size-Induced Oxidation State of Platinum Nanoparticles on Selectivity and Activity in Catalytic Methanol Oxidation in the Gas Phase. Nano Letters, 2013, 13, 2976-2979.	9.1	99
47	Isomerization of n-Hexane Catalyzed by Supported Monodisperse PtRh Bimetallic Nanoparticles. Catalysis Letters, 2013, 143, 907-911.	2.6	20
48	Sum Frequency Generation Vibrational Spectroscopy of Colloidal Platinum Nanoparticle Catalysts: Disordering versus Removal of Organic Capping. Journal of Physical Chemistry C, 2012, 116, 17540-17546.	3.1	40
49	Size and Shape Control of Metal Nanoparticles for Reaction Selectivity in Catalysis. ChemCatChem, 2012, 4, 1512-1524.	3.7	467
50	High Structure Sensitivity of Vapor-Phase Furfural Decarbonylation/Hydrogenation Reaction Network as a Function of Size and Shape of Pt Nanoparticles. Nano Letters, 2012, 12, 5196-5201.	9.1	184
51	Monodisperse Metal Nanoparticle Catalysts: Synthesis, Characterizations, and Molecular Studies Under Reaction Conditions. Topics in Catalysis, 2012, 55, 1257-1275.	2.8	31
52	Reforming of C6 Hydrocarbons Over Model Pt Nanoparticle Catalysts. Topics in Catalysis, 2012, 55, 723-730.	2.8	19
53	Synthesis of Uniformly Sized Manganese Oxide Nanocrystals with Various Sizes and Shapes and Characterization of Their <i>T</i> <sub>1</sub> Magnetic Resonance Relaxivity. European Journal of Inorganic Chemistry, 2012, 2012, 2148-2155.	2.0	71
54	Colloid chemistry of nanocatalysts: A molecular view. Journal of Colloid and Interface Science, 2012, 373, 1-13.	9.4	90

#	Article	IF	CITATIONS
55	Synthesis and biomedical applications of hollow nanostructures. Nano Today, 2009, 4, 359-373.	11.9	370
56	Synthesis of Uniform Hollow Oxide Nanoparticles through Nanoscale Acid Etching. Nano Letters, 2008, 8, 4252-4258.	9.1	210
57	Development of aT1â€Contrast Agent for Magnetic Resonance Imaging Using MnO Nanoparticles. Angewandte Chemie - International Edition, 2007, 46, 5397-5401.	13.8	545
58	Cover Picture: Development of a <i>T</i> <sub>1</sub> â€Contrast Agent for Magnetic Resonance Imaging Using MnO Nanoparticles (Angew. Chem. Int. Ed. 28/2007). Angewandte Chemie - International Edition, 2007, 46, 5247-5247.	13.8	6
59	Sea urchin shaped carbon nanostructured materials: carbon nanotubes immobilized on hollow carbon spheres. Journal of Materials Chemistry, 2006, 16, 2984.	6.7	46
60	Synthesis, Characterization, and Self-Assembly of Pencil-Shaped CoO Nanorods. Journal of the American Chemical Society, 2006, 128, 9753-9760.	13.7	201
61	Large-Scale Synthesis of Hexagonal Pyramid-Shaped ZnO Nanocrystals from Thermolysis of Znâ^'Oleate Complex. Journal of Physical Chemistry B, 2005, 109, 14792-14794.	2.6	128
62	Ultra-large-scale syntheses of monodisperse nanocrystals. Nature Materials, 2004, 3, 891-895.	27.5	3,713